[CANCER RESEARCH 63, 3026–3031, June 15, 2003]

Advances in Brief

Lytic Bone Lesions in Human Neuroblastoma Xenograft Involve Osteoclast Recruitment and Are Inhibited by Bisphosphonate[1]

Yasuyoshi Sohara, Hiroyuki Shimada, Miriam Scadeng, Harvey Pollack, Shinya Yamada, Wei Ye, C. Patrick Reynolds, and Yves A. DeClerck[2]

Departments of Pediatrics, Division of Hematology-Oncology [Y. S., C. P. R., Y. A. D.], Biochemistry and Molecular Biology [Y. A. D.], Pathology [H. S., C. P. R.], Radiology [M. S., H. P.], Neurosurgery [S. Y.], and Preventive Medicine [W. Y.], Childrens Hospital Los Angeles and Keck School of Medicine, University of Southern California, Los Angeles, California 90027

Abstract

Neuroblastoma is the second most common solid tumor in childhood and frequently metastasizes to the bone marrow and the bone matrix. The mechanism involved in bone metastasis and destruction in neuroblastoma is poorly understood. Using a model of bone invasion in immunodeficient mice, we demonstrated that neuroblastoma cells recruited osteoclasts to generate osteolytic lesions and invade the bone matrix. In further support of a contributory role for osteoclasts in neuroblastoma bone invasion, we demonstrated that treatment with the bisphosphonate compound, ibandronate, significantly delayed the progression of osteolytic lesions. The data suggest that bisphosphonates may be clinically effective in the treatment of bone metastases in neuroblastoma.

Introduction

Neuroblastoma is the second most common solid childhood cancer and is responsible for ~15% of childhood cancer deaths (1). This cancer frequently metastasizes to the bone marrow, the liver, the lymph nodes, and the bone. Bone involvement is observed in 55–68% of patients who have metastatic disease at diagnosis (2). Bone lesions caused by metastatic tumor cells are traditionally classified into two processes, *i.e.*, osteolytic and osteoblastic (3, 4). In osteolytic lesions (typically seen in breast cancer and myeloma), tumor cells produce osteoclast-activating factors such as parathyroid hormone-related protein (PTHrP) that stimulate osteoclast maturation and activity. In osteoblastic lesions (frequently reported in prostate cancer), tumor cells produce factors that stimulate osteoblast proliferation, differentiation and bone formation. Often, both osteoclastic and osteoblastic processes are observed. Accordingly, osteoclast inhibitors like bisphosphonate compounds have begun to be used and to show promising results (4–6). In neuroblastoma, however, the mechanisms involved in bone metastasis have not been elucidated, in part because of a lack of adequate preclinical models. As a result, no specific treatments for bone metastasis have been proposed, and bisphosphonates have not been formally tested in patients with neuroblastoma. In the present study, we have developed a model in immunodeficient mice to study the mechanism of bone invasion by human neuroblastoma. By using this model, we demonstrate the crucial role of osteoclasts in this process and provide preclinical data supporting the use of bisphosphonates in the treatment of bone metastases in neuroblastoma.

Materials and Methods

Cell Culture. The human neuroblastoma cell line CHLA-255 was derived from a metastatic lesion in the brain in a patient with recurrent disease after treatment with intensive nonmyeloablative chemotherapy and 13-*cis*-retinoic acid. CHLA-255 cells have amplification of *MYCN*. Cells were cultured in Iscove's modified Dulbecco's medium (Bio-Whittaker, Walkersville, MD) containing 20% fetal bovine serum (Omega Scientific Inc., Tarzana, CA), and supplemented with insulin (5 μg/ml), transferrin (5 μg/ml), and selenium (5 ng/ml; ITS premix; Fisher Scientific, Pittsburgh, PA); penicillin G (100 units/ml); and streptomycin sulfate (100 μg/ml; Irvine Scientific, Santa Ana, CA). The *MYCN*-amplified human neuroblastoma cell lines SK-N-BE (2) and SMS-SAN were previously reported (7, 8). These cells were cultured in RPMI 1640 (Mediatech Inc., Herndon, VA) containing 10% fetal bovine serum supplemented with penicillin G and streptomycin sulfate.

Inoculation of Neuroblastoma Cells in the Femur of Nude Mice. Four-to-six-week-old female BALB/c *nu/nu* mice were purchased from Harlan Sprague Dawley, (St. Louis, MO). Animal housing, care, and procedures were conducted according to the policies of the Institutional Animal Care and Use Committee (IACUC) at Childrens Hospital Los Angeles. Tumor cells were directly injected into the femur by the following method. Mice were anesthetized with an i.p. injection of 2.5% Avertin (300 μl/25 g mice) and placed in a lateral position. The skin covering the right femur and knee was cleaned with Betadine, and a small lateral incision (8–10 mm) was made through the skin at the distal end of the femur. The lateral vastus muscle was split along the septum ~3 mm, and the exposed femoral bone was immobilized with tweezers (Fig. 1*A*). A small hole through the bone and into the bone marrow was made below the patella, between the two femoral condyles, by manually drilling with a 26-gauge sterile needle stabilized with a drill holder. The drilling needle was then removed, and a new needle, fitted to a 50-μl sterile Hamilton syringe (Hamilton Co., Reno, NV), was introduced in the entire marrow cavity until it reached the proximal metaphysis of the femur (Fig. 1*B*). The proper position of the needle inside the bone marrow cavity was verified by transilluminating the femur with a flexible light source. Careful injection of 2 μl of serum-free medium containing 2×10^5 tumor cells was performed over a few seconds, and the needle was then slowly removed. After this procedure was completed, the skin of the wound was closed with formulated cyanoacrylate (Nexaband; Veterinary Products Lab., Phoenix, AZ).

Radiological Examination. High-resolution radiographs were taken under inhalation anesthesia (1.5% isoflurane in 98.5% O_2; Abbott Lab., North Chicago, IL) at weekly intervals with a Faxitron X-ray machine (MX-20; Faxitron X-ray Corp., Wheeling, IL) using a mammography radiographic film/screen combination. This produced high-resolution images with a magnification factor of 5. Each radiograph was evaluated separately by two independent radiologists (M. S. and H. P.) and a consensus was reached. The images were graded using a predetermined grading system. Grade 1 represented a normal bone when compared with the contralateral femur; grade 2 identified the presence of asymmetric, nonprogressive radiolucent lesions limited to the distal femur, associated with the trauma of intra-osseous injection; grade 3 showed asymmetrical osteolytic and progressive radiolucencies extending beyond the distal femur; and grade 4 identified the presence of a pathological fracture of the bone or a breach in the bone cortex.

Histology and Immunohistochemistry. At necropsy, the inoculated femurs were dissected *en bloc* with the acetabulum, the proximal tibia, and the

Received 2/27/03; accepted 4/22/03.

The costs of publication of this article were defrayed in part by the payment of page charges. This article must therefore be hereby marked *advertisement* in accordance with 18 U.S.C. Section 1734 solely to indicate this fact.

[1] Supported by NIH Grant PO1 CA81403 to H. S., C. P. R., and Y. A. D.) and by the T. J. Martell Foundation.

[2] To whom requests for reprints should be addressed, at Division of Hematology-Oncology, Childrens Hospital Los Angeles, 4650 Sunset Boulevard, MS no. 54, Los Angeles, CA 90027. Phone: (323) 669-2150; Fax: (323) 664-9455; E-mail: declerck@hsc.usc.edu.

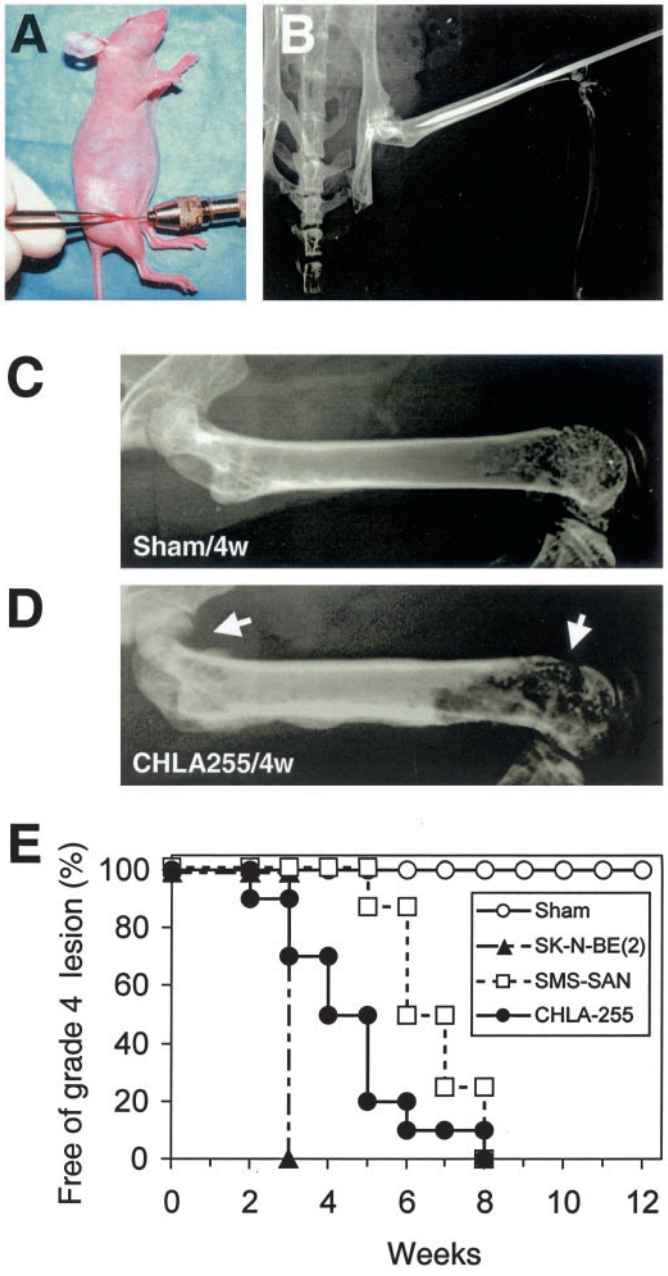

Fig. 1. Bone invasion model in neuroblastoma. *A*, drilling of the femoral bone in an anesthetized mouse. *B*, radiographic image showing the proper position of the injection needle into the bone marrow cavity of the femur. *C* and *D*, radiograph of the femurs obtained 4 weeks after injection of PBS (*C*, *Sham*) or tumor cells (*D*). *White arrows*, pathological fracture of the femoral neck and cortical breach in the distal end of the femur typical of grade 4 lesions. *E*, Kaplan-Meier regression analysis of the percentage of mice free of grade 4 radiological lesions over time. ○, sham group; ▲, SK-N-BE(2); □, SMS-SAN; ●, CHLA-255.

adjacent muscles and were fixed overnight in 10% formaldehyde containing 2% sucrose. The tissues were then decalcified in 0.37% unbuffered formaldehyde containing 5.5% EDTA (pH 6.0–6.5) for 1–2 weeks. After fixation and decalcification, the specimens were embedded in paraffin, and 4-μm sections were obtained and stained with H&E. Detection of osteoclasts in these sections was performed by histochemical staining for TRAP[3] and positive cells, *i.e.*, osteoclasts stained dark red (9). When indicated, mice were injected i.p. 1 h before sacrifice with 2 mg/mouse of BrdUrd. Staining for nuclear BrdUrd was performed by immunohistochemistry as reported previously (10). Staining for the neuroblastoma-specific PGP 9.5 and TH were performed to confirm the presence of neuroblastoma cells in the bone marrow of the femur (11, 12). To quantify the amount of osteoclasts present in the femur, we delineated the surface of the bone in histological section and the surface covered by TRAP-positive cells on digital images, and we used the NIH Image (Ver. 1.62) software to calculate the percentage of surface covered by osteoclasts. To quantify the amount of trabecular bone present in these sections, we measured the area of trabecular bone present in histological sections on digital images generated in Photoshop (version 5.0.2) and used NIH Image software for analysis.

Apoptosis. Apoptosis *in vitro* was determined by fluorescence-activated cell sorting analysis in cell nuclei stained with propidium iodine. The analysis was performed using an EPICS Elite ESP cell sorter (Beckman Coulter, Inc.) and the Expo 32 (version 1.2) software. The percentage of apoptotic cells was determined as the percentage of cells in the sub-G_1-G_0 peak. *In vivo*, we used the TUNEL assay performed with an *in situ* cell death detection kit (Roche Diagnostics GmbH, Mannheim Germany) as per the manufacturer's recommendations.

Treatment with Bisphosphonate. The bisphosphonate compound ibandronate [1-hydroxy-3- (methylpentylamino) propylidine; BM 21.0955] was obtained from Dr. Frieder Bauss, Roche Diagnostics GmbH (Mannheim, Germany). Ibandronate was diluted in sterile PBS at a final concentration of 40 μg/ml and was injected s.c. every day at a dose of 4 μg/mouse. Sterile PBS without ibandronate was similarly injected (100 μl/mouse) in control animals.

Statistical Analysis. The log-rank test was used to compare disease-free time according to the treatment groups. Pair-wise comparison of the treatment groups was also performed using the log-rank test because the *P* for overall test was <0.05. Disease-free time was calculated as the weeks from tumor injection to when a grade 4 radiological lesion was diagnosed in the bone. The Student *t* test was used to compare the number of osteoclasts, the amount of trabecular bone, and the percentage of apoptotic cells between treated and untreated groups.

Results

Neuroblastoma Cells Cause Osteolytic Lesions. Three neuroblastoma cell lines (1×10^5 cells/μl) were each injected into the femur of eight BALB/c *nu/nu* mice. Eight additional mice were given injections of cell-free culture medium (sham group). The mice were X-rayed weekly and were sacrificed when the radiographs revealed the presence of a grade 4 lesion (Fig. 1*D*). The time to develop a grade 4 lesion in all of the mice in each experimental group ranged between 3 and 8 weeks after injection (Fig. 1*E*). The shortest latency period (3 weeks) for the development of a grade 4 lesion was observed in mice that received injections of SK-N-BE (2) cells, and the longest latency period (between 5 and 8 weeks) was observed in mice that received injections of SMS-SAN cells. No grade 3 or 4 lesions were observed in mice of the sham group (Fig. 1*C*). The data indicate that all three of the neuroblastoma cell lines generate osteolytic lesions that can be monitored by X-rays when injected into the femur of immunodeficient mice. We then selected CHLA-255 cells for additional studies.

We also compared the ability of this cell line to form osteolytic bone lesions as a function of different routes of administration. No osteolytic bone lesions were observed when cells (1×10^6) were injected s.c. ($n = 5$), intracardially ($n = 5$), or orthotopically in the left adrenal gland ($n = 5$). However, when cells were injected in the tail vein ($n = 10$), osteolytic lesions in the distal femur were seen at between 7 and 9 weeks in 80% of the mice. However, in seven of these mice, large metastatic tumors in the kidney ($n = 2$), the adrenal gland ($n = 6$), the liver ($n = 1$), and the lung ($n = 1$) developed. The presence of these metastatic tumors prevented us from monitoring the progression of bone lesions because the mice had to be sacrificed. We, therefore, favored local injection in the femur, to be able to examine bone invasion in the absence of formation of distant metastases.

[3] The abbreviations used are: TRAP, tartrate-resistant acid phosphatase; BrdUrd, 5-bromo-2-deoxyuridine triphosphate; TUNEL, terminal deoxynucleotidyl transferase-mediated dUTP-biotin nick end labeling; PGP 9.5, protein gene product 9.5; TH, tyrosine hydroxylase.

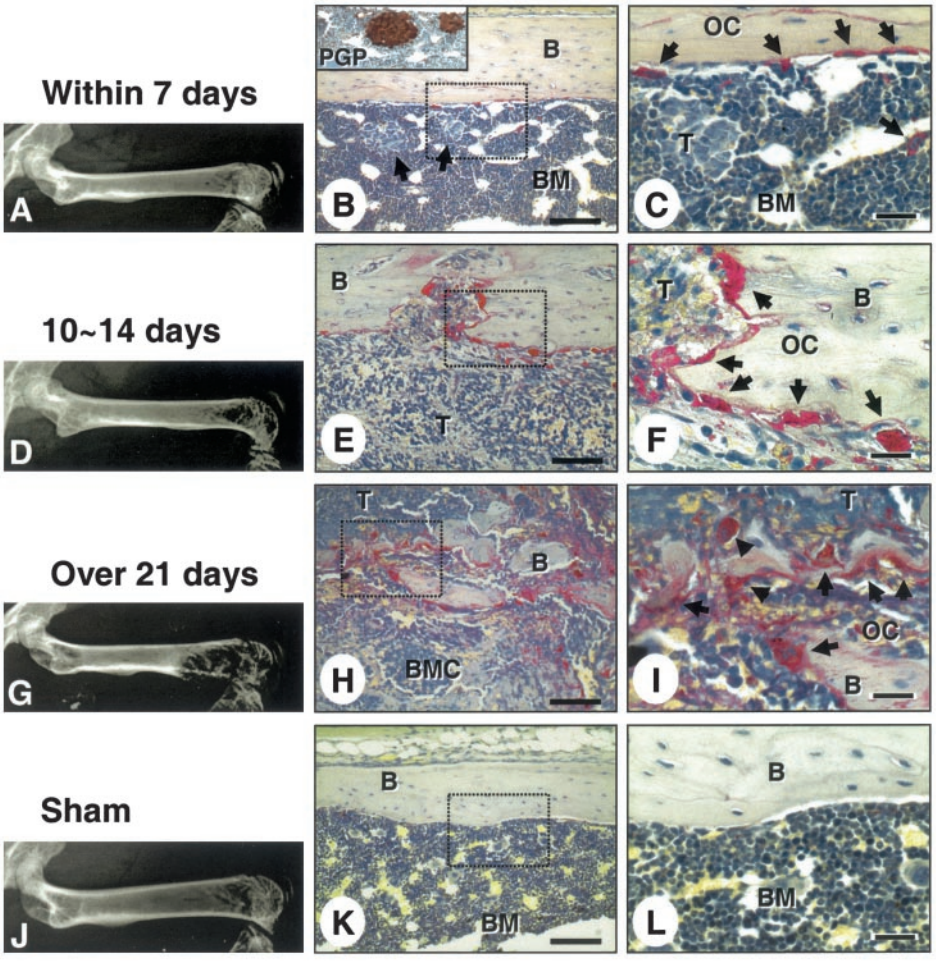

Fig. 2. Time course analysis of bone invasion. *A*, *D*, *G*, and *J*: representative radiographs obtained in mice that were given injections of CHLA-255 cells (*A*, *D*, *G*) or of PBS (*J*), at indicated time. *B*, *C*, *E*, *F*, *H*, *I*, *K*, and *L*: representative histological sections stained for TRAP at indicated time in mice that were given injections of CHLA-255 cells (*B*, *C*, *E*, *F*, *H*, *I*) or of PBS (*K*, *L*) in the right femur. *Scale bars* (*B*, *E*, *H*, *K*), 100 μm; *scale bars* (*C*, *F*, *I*, *L*), 25 μm. *Arrows*, the presence of osteoclasts (*OC*). *B*, bone matrix; *BM*, bone marrow cells; *BMC*, bone marrow cavity; *T*, tumor cells; *PGP*, protein gene product 9.5. The data are representative of a total of 32 mice that were given injections of CHLA-255 cells, with 7 mice examined at day 7, 6 at day 10–14, and 19 between 3 and 8 weeks.

Neuroblastoma Cells Recruit Osteoclasts in the Bone Marrow. Considering the predominantly osteolytic aspect of the femoral bone on X-ray, we speculated that osteoclasts were involved in the formation of bone lesions caused by the intra-osseous injection of neuroblastoma cells. Mice that received injections intra-osseously with CHLA-255 cells were repeatedly X-rayed and sacrificed over time. The femurs were examined histologically for the presence of neuroblastoma cells by immunostaining for PGP 9.5 and TH, and for the presence of osteoclasts by staining for TRAP. Seven days after tumor cell injection, the radiological examination of the femur was always unremarkable (Fig. 2*A*), but the histological analysis of the bone in those mice demonstrated the presence of a few clusters of PGP 9.5- and TH (not shown)-positive tumor cells in the bone marrow space (Fig. 2*B*). TRAP staining of these samples revealed the presence of many osteoclasts located along the intact bone matrix in proximity of the nests of tumor cells (Fig. 2*C*). Between day 10 and day 14 after injection, the radiological examination of the bone revealed the presence of some radiolucent areas in the distal femur that were also seen in mice of the sham group (grade 2 lesion; Fig. 2*D*). On histological sections of the bone of these mice, we observed a marked increase in the number of tumor cells in the bone marrow cavity, and also in the number of TRAP-positive osteoclasts located between tumor cells and trabecular bone (Fig. 2, *E* and *F*). Between 3 and 8 weeks after injection, large and progressive radiolucent areas in the distal end of the femur were observed on radiographs, with often a breach in the bone cortex (grade 3; Fig. 2*G*) and sometimes a pathological fracture in the distal or proximal end of the femur (grade 4; Fig. 1*D*). The histological examination of the femur of these mice showed that the bone marrow cavity was replaced by the tumor cells and that numerous osteoclasts were present at the edge of large areas of bone destruction (Fig. 2, *H* and *I*). These radiological and morphological changes were also observed with SK-N-BE (2) and SMS-SAN cells (data not shown). The radiological and histological examination of the femurs obtained from control mice (sham group) did not show any abnormal radiolucencies in the bones (Fig. 2*J*), nor the presence of osteoclasts in histological sections stained for TRAP, nor any evidence of bone destruction (Fig. 2, *K* and *L*). In summary, primarily osteolytic bone involvement by neuroblastoma cells was associated with recruitment of osteoclasts at the site of tumor invasion.

Treatment with Ibandronate Inhibits the Formation of Osteolytic Lesions. To further demonstrate the active contribution of osteoclasts in neuroblastoma-mediated bone destruction in our xenograft model, we tested the effect of the daily administration of ibandronate (a nitrogen-containing bisphosphonate that inhibits bone resorption) on bone invasion (13). For this experiment, mice were treated either with ibandronate administered the first day of tumor injection (early treatment group) or with ibandronate started 2 weeks after tumor injection (late treatment group). In the control group, mice received a daily injection of PBS. Mice were X-rayed weekly and were sacrificed when a grade 4 lesion was identified on the radiographs (Fig. 3*A*). Treatment with ibandronate resulted in a significant delay of bone invasion, with a median time to develop a grade 4 lesion of 8 weeks (95% CI, 7–9 weeks; $P = 0.003$) and 7 weeks (95% CI, 6/7–9 weeks; $P = 0.02$) for the early and late treatment group, respectively, compared with a median time of 5 weeks in the control group (95% CI, 4–6 weeks). The overall *P*, based on the log-rank test, for comparing

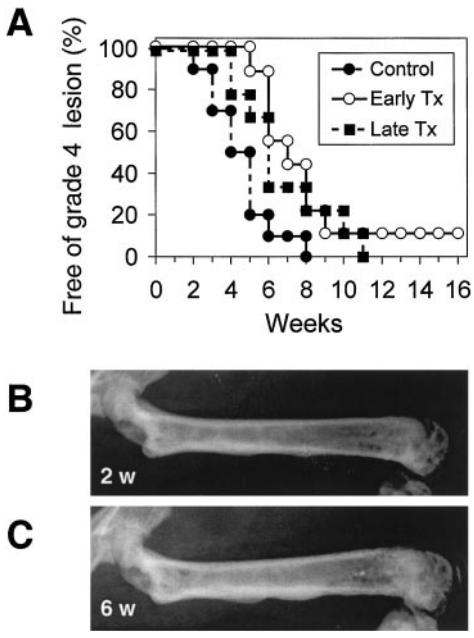

Fig. 3. Treatment with ibandronate. *A*, Kaplan-Meier regression analysis of the percentage of mice free of grade 4 lesion in the three groups; *Tx*, treatment. *B* and *C*, representative radiographs taken 2 weeks (*B*) and 6 weeks (*C*) after tumor cell inoculation in the same mouse treated with ibandronate from day 1.

the three groups was 0.005. The difference between the early and late treatment groups was not statistically significant ($P = 0.55$). In all of the treated mice, the radiological examination of the femur showed a significant amount of osteosclerosis with a marked reduction of osteolysis even 6 weeks after tumor cell injection (Fig. 3, *B* and *C*). Histological examination of the femur of these mice revealed significant differences between the control and treated groups. In the control group, large zones of bone destruction associated with numerous TRAP-positive osteoclasts were typically seen (Fig. 4*A*). When measured along the bone matrix, the bone surface covered with osteoclasts represented 11.5% (±2.67) and 13.0% (±7.71) of the total surface in the early and late treatment groups respectively, compared with 57.0% (±7.54) in the control group ($P < 0.001$). Several osteoclasts were also rounded and detached from the bone matrix in the treated groups (Fig. 4, *B* and *C*). Consistently, the amount of trabecular bone present in bone sections was higher in the treated groups (188.6% ±20.40 and 197.4% ±32.53 of the sham group in the early and late treatment group, respectively) and lower in the control (untreated) group (43.8% ±13.77 of the sham group; $P < 0.001$; Fig. 4*D*). Thus, treatment with ibandronate resulted in a net increase in bone deposition that overcompensated for the bone loss seen in the presence of tumor cells. There were also fewer tumor cells in the femur of ibandronate-treated mice. To determine the mechanism involved, we examined the effect of ibandronate treatment on tumor cell proliferation by BrdUrd immunostaining and on apoptosis by TUNEL assay. The data revealed no difference in the percentage of BrdUrd-positive cells between the control group and the treated groups (Fig. 4*E*). In contrast, there was a significant difference in the number of TUNEL-positive tumor cells between control and treated mice with an average of 41.6 (±37.0) apoptotic cells/mm^2 in the control group and 252.0 (±95.54) apoptotic cells/mm^2 in the treated group (Fig. 4, *F–H*). This effect of ibandronate on apoptosis in tumor cells was likely the result of a direct toxic effect of ibandronate on neuroblastoma cells, because we observed a dose-dependent increase in spontaneous apoptosis in CHLA-255 cells exposed for 72 h to ibandronate *in vitro*. Whereas the percentage of apoptotic cells in the absence or presence of 10^{-5} M of ibandronate was 0.3%, the percentage of apoptotic cells increased to 16.8% and 45.7% in the presence of 10^{-4} and 10^{-3} M of ibandronate, respectively. In summary, treatment with ibandronate decreased the number of osteoclasts present in bone marrow, increased the amount of bone deposition, and increased apoptosis in tumor cells.

Discussion

Bone metastasis is an important factor of morbidity and mortality in patients with neuroblastoma for which, with the exception of local palliative irradiation, there is no effective treatment (14). To test agents of potential therapeutic efficacy, we have developed a preclinical murine model to study neuroblastoma bone metastasis. We opted for the injection of tumor cells directly into the femoral bone marrow cavity (15, 16). Many investigators have used intraventricular, i.v., or s.c. injections of tumor cells derived from breast and prostate cancers and also from neuroblastoma to study bone metastasis (11, 17–20). These models have the advantage of recapitulating the hematogenous spread of tumor cells to the bone marrow cavity and the invasion of the bone matrix by tumor cells established in the bone marrow. Often, however, in these models, organs other than the bone are colonized by metastatic tumor cells, causing premature death before a full evaluation of bone invasion is possible. This was also the case with CHLA-255 cells which, when injected i.v., formed large metastatic tumors in addition to osteolytic lesions (12). A substantial advantage of our model is, therefore, that it allows the study of bone invasion over time, and the examination of the effect of therapeutic intervention restricted to bone invasion (like ibandronate). These studies would not have been possible if distant metastases had developed.

Our model raises the question of the potential contribution of the needle trauma in the formation of the bone lesions. It is unlikely that the trauma associated with the needle played any role because osteolytic lesions were also observed in the proximal end of the femur away from the site of trauma. It should also be noticed that CHLA-255 cells formed similar osteolytic lesions in the distal end of the femur when injected i.v., thus in the absence of any local trauma to the bone. To our knowledge, local trauma has not been reported as a predisposing factor for neuroblastoma bone metastasis.

The mechanisms by which neuroblastoma cells cause bone lesions have not been fully elucidated. In one study, immmunodeficient mice that were given injections s.c. of NB19 human neuroblastoma cells were shown to develop osteolytic lesions in the tibia or the femur in 70% of the cases (18). The histological analysis of the bones indicated a decrease in the volume of the trabecular bone with microscopic invasion by tumor cells, but the role of osteoclasts in these lesions was not evaluated. In support for an involvement of osteoclasts was the observation in the same study, that when cocultured with bone marrow stromal cells, NB19 neuroblastoma cells stimulated the expression of the receptor activator of nuclear factor κB ligand (RANKL) by bone marrow stromal cells. RANKL is a type II transmembrane protein that stimulates osteoclast maturation and activity (21). The marked and rapid increase in osteoclasts observed over time in our model demonstrates that neuroblastoma cells actively recruit osteoclasts *in vivo*.

Further supporting a role for osteoclasts in bone invasion is our observation that the administration of a bisphosphonate compound, ibandronate, inhibits osteoclasts recruitment, bone resorption, and bone invasion by tumor cells (3, 5, 6). Ibandronate belongs to the highly potent nitrogen-containing bisphosphonates, whose mode of action is by interaction with the mevalonate pathway and by inhibition of geranyl geranyl diphosphate synthase that is required for osteoclast formation (22, 23). When ibandronate was administered to mice with osteolytic lesions postinoculation of MDA-MB-231 human breast

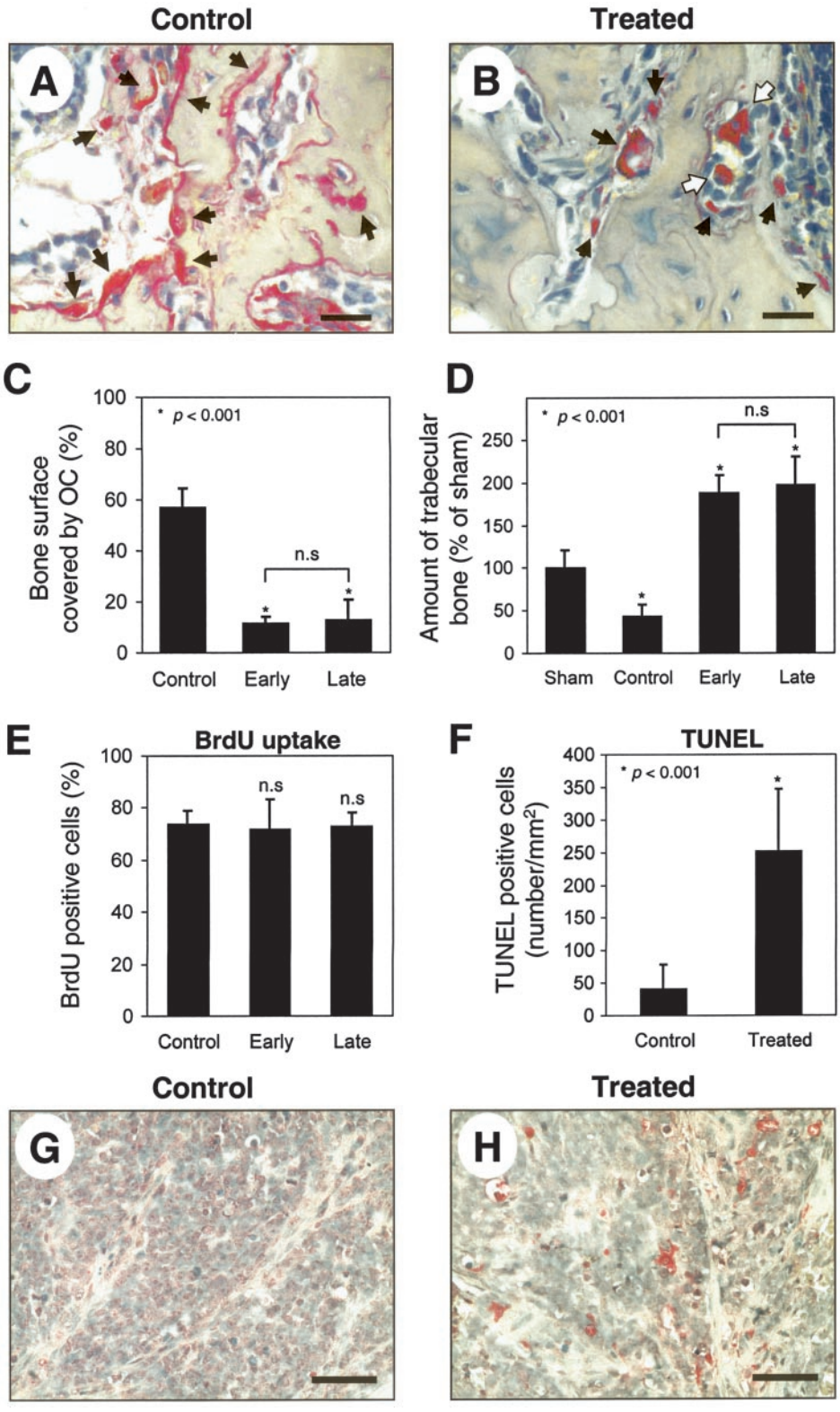

Fig. 4. Effect of ibandronate treatment on osteoclastogenesis, bone resorption, tumor cell proliferation, and apoptosis. *A* and *B*, representative histological sections stained for TRAP in a control (*A*) and a treated (*B*) tumor; *bar*, 25 μm. *Filled arrows*, osteoclasts; *open arrows*, round osteoclasts detached from the bone matrix. *C*, amount of osteoclasts (OC) that are present, calculated as a percentage of the surface of the bone matrix covered by osteoclasts. The data represent the mean ($\pm$SD) of 12 fields in each group with two to three mice analyzed in each group. *D*, amount of trabecular bone. The data represent the relative mean percentage of trabecular bone ($\pm$SD) for each group compared with the amount of bone in the sham group (100%). There were nine mice in the sham group, four in the control group, six in the early treatment group, and seven in the late treatment group. *E*, BrdUrd staining. The data represent the mean percentage of BrdUrd-positive cells ($\pm$SD) in each group. There were three mice in each group with four sections examined in each mouse. *F*, apoptosis. The data represent the mean number of apoptotic cells/mm^2 ($\pm$SD) in control and treated mice. *G* and *H*, representative histological sections stained for TUNEL; *bar*, 50 μm.

cancer cells, a decrease not only in bone lesions but also in tumor burden was observed (24), and this latter effect involved a direct effect of ibandronate on tumor cell apoptosis (17). Consistent with this observation, we noticed in mice treated with ibandronate, a decrease in tumor burden associated with a significant increase in the number of apoptotic tumor cells, and *in vitro* we documented an increase in spontaneous apoptosis in the presence of ibandronate concentrations of 10^{-4} and 10^{-3} M, similar to a previous report (17). In contrast, tumor cell proliferation was not affected by treatment with ibandronate.

Bisphosphonates have been recognized as an important class of therapeutic agents for diseases associated with bone loss such as osteoporosis and Paget's disease and have begun to be used to treat breast and prostate cancers that have metastasized to bones (25). In neuroblastoma, these agents have not been tested to date because the

mechanism of bone invasion has not been understood. Here we provide convincing *in vivo* evidence that osteoclasts are recruited by neuroblastoma cells that are present in the bone marrow and are involved in the formation of osteolytic lesions. These data suggest that bisphosphonates could be clinically useful in patients with neuroblastoma who have developed bone metastases.

Acknowledgments

We thank Jackie Rosenberg for typing the manuscript. We thank Morgan Woo, Sue Wang, Minerva Mongeotti, Katie Lacina, and George McNamara for their assistance in the histological analysis of the data and for the microscopic images.

References

1. Matthay, K. K., Villablanca, J. G., Seeger, R. C., Stram, D. O., Harris, R. E., Ramsay, N. K., Swift, P., Shimada, H., Black, C. T., Brodeur, G. M., Gerbing, R. B., and Reynolds, C. P. Treatment of high-risk neuroblastoma with intensive chemotherapy, radiotherapy, autologous bone marrow transplantation, and 13-*cis*-retinoic acid. Children's Cancer Group. N. Engl. J. Med., *341:* 1165–1173, 1999.
2. Dubois, S. G., Kalika, Y., Lukens, J. N., Brodeur, G. M., Seeger, R. C., Atkinson, J. B., Haase, G. M., Black, C. T., Perez, C., Shimada, H., Gerbing, R., Stram, D. O., and Matthay, K. K. Metastatic sites in stage IV and IVS neuroblastoma correlate with age, tumor biology, and survival. J. Pediatr. Hematol. Oncol., *21:* 181–189, 1999.
3. Mundy, G. R., Yoneda, T., and Hiraga, T. Preclinical studies with zoledronic acid and other bisphosphonates: impact on the bone microenvironment. Semin. Oncol., *28:* 35–44, 2001.
4. Mundy, G. R. Metastasis to bone: causes, consequences and therapeutic opportunities. Nat. Rev. Cancer, *2:* 584–593, 2002.
5. Diel, I. J., Solomayer, E. F., and Bastert, G. Bisphosphonates and the prevention of metastasis: first evidences from preclinical and clinical studies. Cancer (Phila.), *88:* 3080–3088, 2000.
6. Rodan, G. A., and Martin, T. J. Therapeutic approaches to bone diseases. Science (Wash. DC), *289:* 1508–1514, 2000.
7. Sugiura, Y., Shimada, H., Seeger, R. C., Laug, W. E., and DeClerck, Y. A. Matrix metalloproteinases-2 and -9 are expressed in human neuroblastoma: contribution of stromal cells to their production and correlation with metastasis. Cancer Res., *58:* 2209–2216, 1998.
8. Reynolds, C. P., Biedler, J. L., Spengler, B. A., Reynolds, D. A., Ross, R. A., Frenkel, E. P., and Smith, R. G. Characterization of human neuroblastoma cell lines established before and after therapy. J. Natl. Cancer Inst. (Bethesda), *76:* 375–387, 1986.
9. Takahashi, N., Yamana, H., Yoshiki, S., Roodman, G. D., Mundy, G. R., Jones, S. J., Boyde, A., and Suda, T. Osteoclast-like cell formation and its regulation by osteotropic hormones in mouse bone marrow cultures. Endocrinology, *122:* 1373–1382, 1988.
10. Taylor, G., Lehrer, M. S., Jensen, P. J., Sun, T. T., and Lavker, R. M. Involvement of follicular stem cells in forming not only the follicle but also the epidermis. Cell, *102:* 451–461, 2000.
11. Wirnsberger, G. H., Becker, H., Ziervogel, K., and Hofler, H. Diagnostic immunohistochemistry of neuroblastic tumors. Am. J. Surg. Pathol., *16:* 49–57, 1992.
12. Goto, S, Sun, B., Shimada, H., and Reynolds, C. P. Defining the natural history of a metastatic human neuroblastoma model with PGP 9.5 immunohistochemistry. Proc. Amer. Assoc. Cancer Res. *43:* 1014. 2002.
13. Muhlbauer, R. C., Bauss, F., Schenk, R., Janner, M., Bosies, E., Strein, K., and Fleisch, H. BM 21.0955, a potent new bisphosphonate to inhibit bone resorption. J. Bone Miner. Res., *6:* 1003–1011, 1991.
14. Paulino, A. C. Palliative radiotherapy in children with neuroblastoma. Pediatr. Hematol. Oncol., *20:* 111–117, 2003.
15. Yang, J., Fizazi, K., Peleg, S., Sikes, C. R., Raymond, A. K., Jamal, N., Hu, M., Olive, M., Martinez, L. A., Wood, C. G., Logothetis, C. J., Karsenty, G., and Navone, N. M. Prostate cancer cells induce osteoblast differentiation through a Cbfa1-dependent pathway. Cancer Res., *61:* 5652–5659, 2001.
16. Lee, Y. P., Schwarz, E. M., Davies, M., Jo, M., Gates, J., Zhang, X., Wu, J., and Lieberman, J. R. Use of zoledronate to treat osteoblastic versus osteolytic lesions in a severe-combined-immunodeficient mouse model. Cancer Res., *62:* 5564–5570, 2002.
17. Hiraga, T., Williams, P. J., Mundy, G. R., and Yoneda, T. The bisphosphonate ibandronate promotes apoptosis in MDA-MB-231 human breast cancer cells in bone metastases. Cancer Res., *61:* 4418–4424, 2001.
18. Michigami, T., Ihara-Watanabe, M., Yamazaki, M., and Ozono, K. Receptor activator of nuclear factor κB ligand (RANKL) is a key molecule of osteoclast formation for bone metastasis in a newly developed model of human neuroblastoma. Cancer Res., *61:* 1637–1644, 2001.
19. Yoneda, T., Michigami, T., Yi, B., Williams, P. J., Niewolna, M., and Hiraga, T. Actions of bisphosphonate on bone metastasis in animal models of breast carcinoma. Cancer (Phila.), *88:* 2979–2988, 2000.
20. Papapoulos, S. E., Hamdy, N. A., and van der Pluijm, G. Bisphosphonates in the management of prostate carcinoma metastatic to the skeleton. Cancer (Phila.), *88:* 3047–3053, 2000.
21. Burgess, T. L., Qian, Y., Kaufman, S., Ring, B. D., Van, G., Capparelli, C., Kelley, M., Hsu, H., Boyle, W. J., Dunstan, C. R., Hu, S., and Lacey, D. L. The ligand for osteoprotegerin (OPGL) directly activates mature osteoclasts. J. Cell Biol., *145:* 527–538, 1999.
22. Coxon, F. P., Helfrich, M. H., Van't Hof, R., Sebti, S., Ralston, S. H., Hamilton, A., and Rogers, M. J. Protein geranylgeranylation is required for osteoclast formation, function, and survival: inhibition by bisphosphonates and GGTI-298. J. Bone Miner. Res., *15:* 1467–1476, 2000.
23. Rogers, M. J., Gordon, S., Benford, H. L., Coxon, F. P., Luckman, S. P., Monkkonen, J., and Frith, J. C. Cellular and molecular mechanisms of action of bisphosphonates. Cancer (Phila.), *88:* 2961–2978, 2000.
24. Sasaki, A., Alcalde, R. E., Nishiyama, A., Lim, D. D., Mese, H., Akedo, H., and Matsumura, T. Angiogenesis inhibitor TNP-470 inhibits human breast cancer osteolytic bone metastasis in nude mice through the reduction of bone resorption. Cancer Res., *58:* 462–467, 1998.
25. Rosen, L. S., Gordon, D., Antonio, B. S., Kaminski, M., Howell, A., Belch, A., Mackey, J. A., Apffelstaedt, J., Tfrin, M., Hussein, M., Coleman, R. E., Reitsma, D. J., Seaman, J. J., Chen, B. L., and Ambros, Y. Zoledronic acid versus pamidronate in the treatment of skeletal metastases in patients with breast cancer or osteolytic lesions of multiple myeloma: a Phase III, double-blind, comparative trial. Cancer J., *7:* 377–387, 2001.